

Low-temperature physical properties of $R_5\text{Ir}_4\text{Si}_{10}$ ($R = \text{Dy}, \text{Ho}, \text{Er}, \text{Tm}, \text{and Yb}$) compounds

H. D. Yang

Department of Physics, National Sun Yat-sen University, Kaohsiung, Taiwan 804 24, Republic of China

P. Klavins and R. N. Shelton

Department of Physics, University of California, Davis, Davis, California 95616

(Received 2 July 1990)

Results on the static magnetic susceptibility and dc electrical resistivity of $R_5\text{Ir}_4\text{Si}_{10}$ ($R = \text{Dy} - \text{Yb}$) compounds are presented. In addition, measurements of the ac magnetic susceptibility and resistivity at high pressure and heat capacity for $\text{Tm}_5\text{Ir}_4\text{Si}_{10}$ are also reported. Magnetic-ordering temperatures for these isostructural compounds range from 0.8 to 5 K, with $\text{Tm}_5\text{Ir}_4\text{Si}_{10}$ displaying two magnetic transitions. All these compounds exhibit an anomalous temperature dependence of the resistivity which may be attributed to charge-density-wave formation.

I. INTRODUCTION

Rare-earth-transition-metal ternary compounds exhibit a great variety of unusual phenomena.¹ In particular, the interplay between superconductivity and long-range magnetic order in the rhombohedral rare-earth molybdenum chalcogenides $R\text{Mo}_6\text{S}_8$ (Ref. 2) and the tetragonal rare-earth rhodium borides RRh_4B_4 (Ref. 3) has been a subject of extensive study. More recently, three rare-earth-transition-metal silicides, $R_2\text{Fe}_3\text{Si}_5$,^{4,5} $R_5\text{Co}_4\text{Si}_{10}$,⁶ and $RCu_2\text{Si}_2$,⁷ have also received much attention due to the relatively high superconducting transition temperatures ($\text{Lu}_2\text{Fe}_3\text{Si}_5$, $T_c = 6.2$ K; $\text{Sc}_5\text{Co}_4\text{Si}_{10}$, $T_c = 4.9$ K) observed even in the presence of magnetic 3d transition elements (30 mol % iron and 21 mol % Co) for the first two systems and superconductivity involving electrons with an enormous effective mass (CeCu_2Si_2 , $m^*/m \sim 200$, $T_c = 0.5$ K) for the last system.

Reports of large pressure effects on T_c in $\text{Y}_2\text{Fe}_3\text{Si}_5$,⁸ reentrant,⁹ and pressure-induced superconductivity destroyed by long-range antiferromagnetic order in $\text{Tm}_2\text{Fe}_3\text{Si}_5$,¹⁰ complicated multiple magnetic phase transitions in $\text{Sm}_2\text{Fe}_3\text{Si}_5$, $\text{Tb}_2\text{Fe}_3\text{Si}_5$, and $\text{Er}_2\text{Fe}_3\text{Si}_5$ shown in heat-capacity measurements,¹¹ anomalous pressure effects on T_c ,¹² and unconventional temperature dependence of resistivity and magnetic susceptibility in $\text{Lu}_5\text{Ir}_4\text{Si}_{10}$ (Ref. 13) all provide motivation for our present study of the low-temperature physical properties of the $R_5\text{Ir}_4\text{Si}_{10}$ system as a means of better understanding the nature of superconductivity, magnetic order, and electronic phase transition in these materials.

The rare-earth iridium silicides $R_5\text{Ir}_4\text{Si}_{10}$ ($R = \text{Dy}, \text{Ho}, \text{Er}, \text{and Tm}$) are formed in the $\text{Sc}_5\text{Co}_4\text{Si}_{10}$ -type structure. Magnetic-ordering temperatures, $T_N = 5.0$ K (Dy), 1.5 K (Ho), 2.3 K (Er), and 1.0 K (Tm) have been reported previously.¹⁴ In this work, we investigate the static magnetic susceptibility and electrical resistivity for $R_5\text{Ir}_4\text{Si}_{10}$, including $\text{Yb}_5\text{Ir}_4\text{Si}_{10}$, as well as the resistivity and ac susceptibility under high pressure and heat capacity for $\text{Tm}_5\text{Ir}_4\text{Si}_{10}$. This work focuses on the interplay among

valence fluctuations, superconductivity, and magnetic order in these compounds.

II. EXPERIMENTAL DETAILS

Samples of $R_5\text{Ir}_4\text{Si}_{10}$ ($R = \text{Dy} - \text{Tm}$) were prepared by arc melting stoichiometric mixtures of high-purity elements in a Zr-gettered argon atmosphere. The resulting ingots were turned over and remelted several times to promote homogeneity. The samples were then sealed in quartz ampules with about 160 Torr of argon and annealed at 1250 °C for one day followed by three days at 1050 °C. The sample of $\text{Yb}_5\text{Ir}_4\text{Si}_{10}$ was prepared with an excess of Yb over that required for a stoichiometric sample due to the relatively low boiling point and high vapor pressure of Yb. A sample in "as-cast" form was used, since the annealing process resulted in a significant loss of Yb. The lattice parameters of tetragonal cell (space group $P4/mbm$) were determined from powder x-ray diffraction patterns by the method of least squares using 20–24 reflections including an internal silicon standard ($a = 5.43083$ Å). No impurity reflections were observed. Static-magnetic-susceptibility data were taken in a commercial superconducting quantum interference device (SQUID) magnetometer¹⁵ in a field of 2 kOe. The dc resistivity at ambient pressure and the ac resistivity at high pressure were measured on samples of rectangular parallelepipeds of approximate dimensions $1 \times 1 \times 5$ and $2 \times 2 \times 1$ mm³ using a four-probe method. High-pressure measurements of T_N and the electrical resistivity were done using a piston-cylinder-type hydrostatic-pressure clamp.¹⁶ Low-temperature heat-capacity measurements were performed using a semiadiabatic heat-pulse-type calorimeter. Details of measurement technique may be found in Ref. 17.

III. RESULTS AND DISCUSSION

A. Crystallography and magnetic properties

The lattice parameters and unit-cell volumes of $R_5\text{Ir}_4\text{Si}_{10}$ ($R = \text{Dy}, \text{Ho}, \text{Er}, \text{Tm}, \text{Yb}, \text{and Lu}$) are listed in

Table I, which are basically in agreement with those found in the literature.¹⁴ It should be noted that our data on $\text{Yb}_5\text{Ir}_4\text{Si}_{10}$ are an additional contribution to this literature. The variation in the lattice parameters and unit-cell volumes with rare earth are shown in Fig. 1. The plot indicates that all the rare-earth ions in these compounds are trivalent at room temperature. In fact, the a and c values decrease, going from Dy to Lu, by approximately 0.8% and 1.6%, respectively. These contractions are about the same order of magnitude as those found for the $R_2\text{Fe}_3\text{Si}_5$ series. These results also reflect one crystallographic feature of this structure, namely, that the c parameter is equal to the height of the $R_6\text{Si}$ trigonal prism and is thus directly coupled to the rare-earth radius. The a parameter does not vary as rapidly as c , since the former is determined by both the rare-earth radius and the size of the transition-metal atom. This observation on crystallographic stability correlates with the fact that this structure forms only with rare earths of size equal to or less than that of Dy.

The results of magnetic measurements on $R_5\text{Ir}_4\text{Si}_{10}$ ($R = \text{Dy}, \text{Ho}, \text{Er}, \text{Tm}, \text{and Yb}$) silicides are presented in Table I, with the reciprocal molar magnetic susceptibility as a function of temperature taken from 2.6 to 300 K displayed in Fig. 2. The paramagnetic susceptibility of these compounds closely obeys the Curie-Weiss law at high temperature ($T > 50$ K) and the magnetic parameters are obtained from a least-squares fit with the general equation

$$\chi_m = \frac{N_A(\mu_{\text{eff}})^2}{3k_B(T - \Theta)} + \chi_0, \quad (1)$$

where N_A is the Avogadro number, k_B is the Boltzmann constant, Θ is the asymptotic Curie temperature, and χ_0 corresponds to the temperature-independent term including the diamagnetic core term (χ_{dia}), the Pauli susceptibility of the conduction electrons (χ_{Pauli}), and the diamagnetic orbital contribution due to the conduction electrons (χ_{Landau}). The calculated effective magnetic moments are slightly larger than those expected for R^{3+} free ions. This observation has also been made for the $R_2\text{Fe}_3\text{Si}_5$ compounds and indicates that there may be a small contribution from the transition-element sublattice. A slight deviation of the magnetic susceptibility (more noticeable in $\text{Yb}_5\text{Ir}_4\text{Si}_{10}$) from the Curie-Weiss law below 50 K suggests the presence of crystal-field effects. The magnetic-ordering temperatures T_N of these compounds

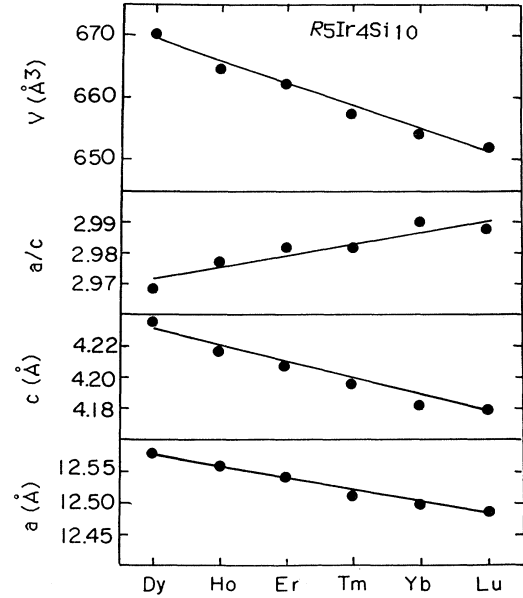


FIG. 1. Variation in the lattice parameters a/c and unit-cell volume for $R_5\text{Ir}_4\text{Si}_{10}$ with rare earths $R = \text{Dy-Lu}$. Lines are guides to the eye. Error bars are included in the symbols.

($R = \text{Dy-Tm}$) are defined as the temperature corresponding to a cusplike anomaly in the χ_{ac} -versus- T plot and given in Table I. A typical anomaly is seen in the inset of Fig. 2 for $\text{Dy}_5\text{Ir}_4\text{Si}_{10}$. The small negative values of Θ and the coexistence of superconductivity and magnetic order in $(\text{Sc}_{1-x}\text{Dy}_x)_5\text{Ir}_4\text{Si}_{10}$ solid solutions¹⁸ indicate that these materials order antiferromagnetically. In contrast, no anomaly is observed above 52 mK at ambient pressure or above 1.2 K at the pressure of 18 kbar for $\text{Yb}_5\text{Ir}_4\text{Si}_{10}$. Valence fluctuations at low temperature may be important for $\text{Yb}_5\text{Ir}_4\text{Si}_{10}$ because its magnetic susceptibility deviates significantly from the Curie-Weiss law as the temperature is lowered below 70 K.

B. Electrical resistivity

The normalized-resistivity data as a function of temperature between 2.6 and 300 K for $R_5\text{Ir}_4\text{Si}_{10}$ ($R = \text{Dy-Yb}$) are presented in Fig. 3. One cusp for $\text{Dy}_5\text{Ir}_4\text{Si}_{10}$, $\text{Ho}_5\text{Ir}_4\text{Si}_{10}$, and $\text{Yb}_5\text{Ir}_4\text{Si}_{10}$ and two distinct cusps for $\text{Er}_5\text{Ir}_4\text{Si}_{10}$ and $\text{Tm}_5\text{Ir}_4\text{Si}_{10}$ are observed. We note the rapid rise in resistivity between 60 and 70 K for $\text{Er}_5\text{Ir}_4\text{Si}_{10}$ and between 25 and 40 K for $\text{Tm}_5\text{Ir}_4\text{Si}_{10}$.

TABLE I. Crystallographic and magnetic parameters for some ternary silicides $R_5\text{Ir}_4\text{Si}_{10}$.

Compound	a (Å)	c (Å)	a/c	V (Å ³)	$\mu_{\text{eff}}(\mu_B)$		Θ (K)	T_N (K)
					Expt.	Theor.		
$\text{Yb}_5\text{Ir}_4\text{Si}_{10}$	12.503(3)	4.182(2)	2.990	653.74	4.53	4.54	-58.8	a
$\text{Tm}_5\text{Ir}_4\text{Si}_{10}$	12.513(2)	4.197(1)	2.982	657.14	8.05	7.55	-27.1	1.9
$\text{Er}_5\text{Ir}_4\text{Si}_{10}$	12.540(2)	4.208(1)	2.981	661.80	9.79	9.59	0.6	3.0
$\text{Ho}_5\text{Ir}_4\text{Si}_{10}$	12.558(2)	4.218(1)	2.977	665.10	11.27	10.58	-13.2	2.0
$\text{Dy}_5\text{Ir}_4\text{Si}_{10}$	12.577(2)	4.237(1)	2.968	670.16	10.69	10.63	-5.9	5.0

^aNot observed down to 52 mK.

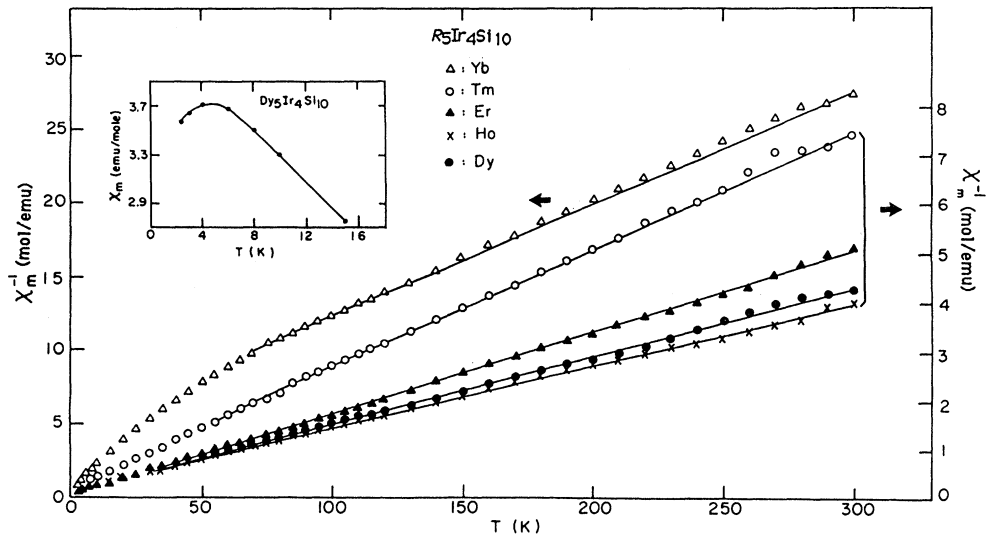


FIG. 2. Reciprocal molar magnetic susceptibility as a function of temperature for $R_5\text{Ir}_4\text{Si}_{10}$ ($R = \text{Dy}-\text{Yb}$). Inset shows the magnetic susceptibility of $\text{Dy}_5\text{Ir}_4\text{Si}_{10}$ at low temperature.

The temperature T_0 at which the cusp occurs for each rare-earth compound is plotted in Fig. 4. The anomalies in these compounds have the same nature as that in $\text{Lu}_5\text{Ir}_4\text{Si}_{10}$ for the following reasons.

(1) Except for $\text{Yb}_5\text{Ir}_4\text{Si}_{10}$, T_0 decreases just like the volume contraction seen in Fig. 1. This is also consistent with the pressure effect on this kind of electronic phase transition, which has been studied for $\text{Lu}_5\text{Ir}_4\text{Si}_{10}$.

(2) In Fig. 5, we see the smooth change of T_0 across the $(\text{Lu}_{1-x}\text{Er}_x)_5\text{Ir}_4\text{Si}_{10}$ system, thus maintaining the resistive anomaly.

(3) In work¹⁹ on the isostructural pseudoternary series $(\text{Lu}_{0.9}\text{R}_{0.1})_5\text{Ir}_4\text{Si}_{10}$ ($R = \text{Dy}-\text{Tm}$), the sudden jump in T_c

at high pressure is retained, thus providing a strong argument that this mechanism was not destroyed by magnetic-rare-earth substitution in these cases. We can ascribe this to the same type of phase transition also formed in the pure ternary compounds $R_5\text{Ir}_4\text{Si}_{10}$ ($R = \text{Dy}-\text{Yb}$).

In Fig. 4, the $T_0 = 56$ K of $\text{Yb}_5\text{Ir}_4\text{Si}_{10}$ lies significantly below the line that connects the data points for the other compounds. This deviation may be due to a valence fluctuation of Yb at low temperature. From this point of view, we conclude that the volume change is not as dominant an influence on the anomaly as the electronic-configuration difference. The two anomalies in resistivity

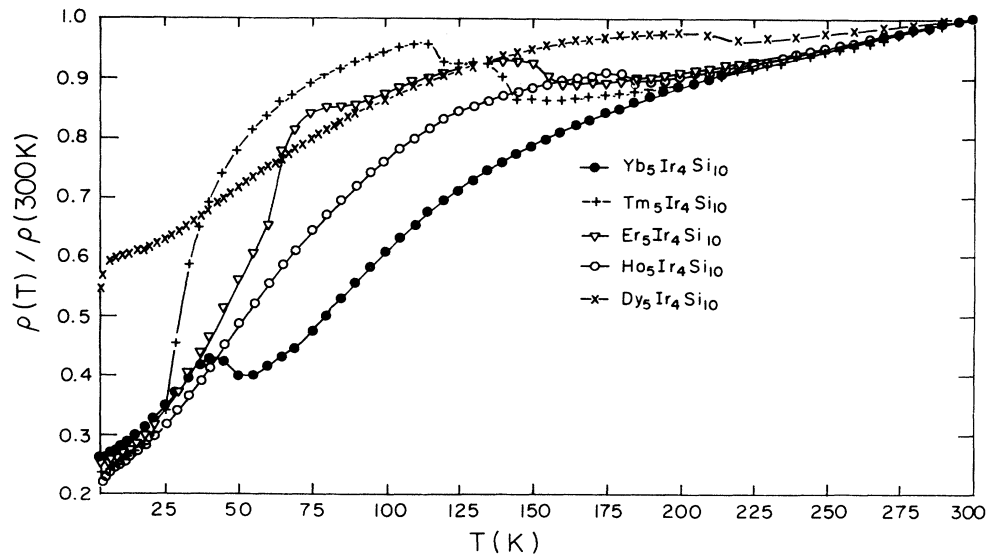


FIG. 3. Normalized resistivity as a function of temperatures between 2.6 and 300 K for $R_5\text{Ir}_4\text{Si}_{10}$ ($R = \text{Dy}-\text{Yb}$).

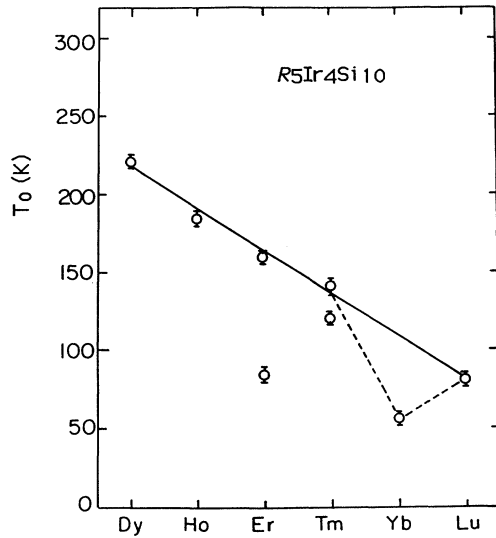


FIG. 4. The resistive-anomaly temperature T_0 for $R_5\text{Ir}_4\text{Si}_{10}$ ($R = \text{Dy-Lu}$).

for $\text{Er}_5\text{Ir}_4\text{Si}_{10}$ and $\text{Tm}_5\text{Ir}_4\text{Si}_{10}$ reflect the presence of more complex electronic phase transitions. This kind of phenomena was seen in the quasi-one-dimensional compound NbSe_3 (Ref. 20) and the layered dichalcogenide compound TaS_2 .^{21,22}

C. Pressure effect in $\text{Tm}_5\text{Ir}_4\text{Si}_{10}$

For $\text{Tm}_5\text{Ir}_4\text{Si}_{10}$, the ac magnetic susceptibility versus temperature at different applied pressures is shown in Fig. 6. The temperature at which the cusp occurs increases only slightly with pressure; however, the slope and magnitude of the χ_{ac} signal depend strongly on the

pressure. The cusp is not as pronounced at ambient and high pressures (20 kbar) as at intermediate pressures (14–15 kbar). This may indicate that the strength or the type of the magnetic transition are different under various pressures. In fact, as the temperature is further lowered at ambient pressure in a dilution refrigerator, another sharper cusp is found at 0.82 K. Comparing these two anomalies in shape and amplitude, we speculate that this compound orders antiferromagnetically at 1.8 K and then ferromagnetically at 0.82 K. This idea is generally supported by the heat-capacity data (see next section), and should be confirmed by other experiments, such as neutron diffraction.

Normalized-resistivity-versus-temperature data between 4 and 300 K at four different pressures for $\text{Tm}_5\text{Ir}_4\text{Si}_{10}$ are presented in Fig. 7. The positions of the two anomalies decrease monotonically by the application of pressure at the rate $(dT_0/dp)_{p=0} = -1.2$ K/kbar for the higher and -1.4 K/kbar for the lower. The anomalies are also depressed in height and become broader in shape with pressure. Comparing the two results shown in Figs. 6 and 7, we find that pressure affects the electronic-phase-transition temperature T_0 and the magnetic-ordering temperature T_N in $\text{Tm}_5\text{Ir}_4\text{Si}_{10}$ very differently.

D. Heat capacity for $\text{Tm}_5\text{Ir}_4\text{Si}_{10}$

The low-temperature heat-capacity data between 0.6 and 30 K for $\text{Tm}_5\text{Ir}_4\text{Si}_{10}$ are presented in Fig. 8. Two distinct maxima at 0.86 and 1.91 K, shown in the inset of Fig. 8, indicate the presence of two magnetic phase transitions. This is consistent with the magnetic-susceptibility measurement as determined by a low-frequency (~ 25 Hz) ac inductance technique. We note that the sizes and the shapes of the maxima shown in the inset of Fig. 8 are completely different. This may reflect

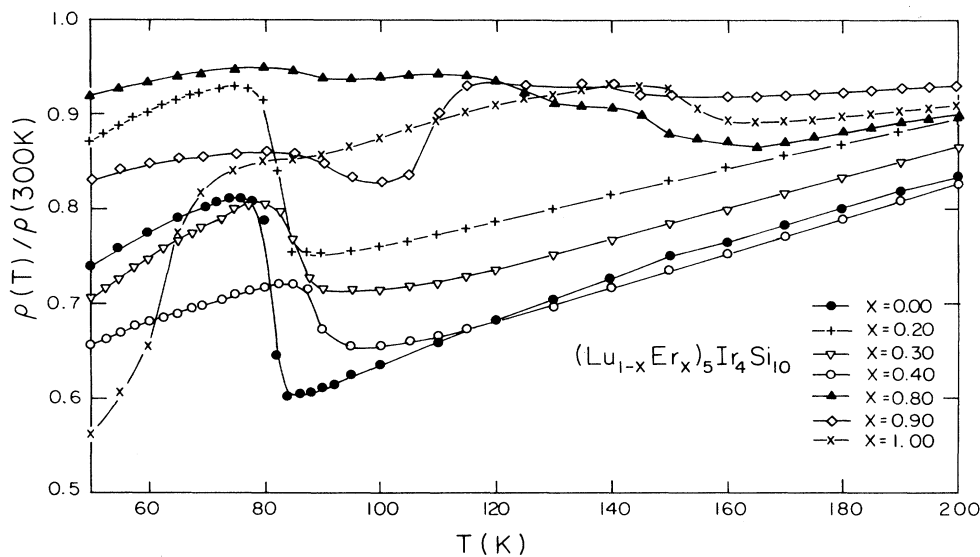


FIG. 5. Normalized resistivity as a function of temperature between 50 and 200 K for the pseudoternary system $(\text{Lu}_{1-x}\text{Er}_x)_5\text{Ir}_4\text{Si}_{10}$ ($x = 0, 0.2, 0.3, 0.4, 0.8, 0.9, \text{ and } 1.0$).

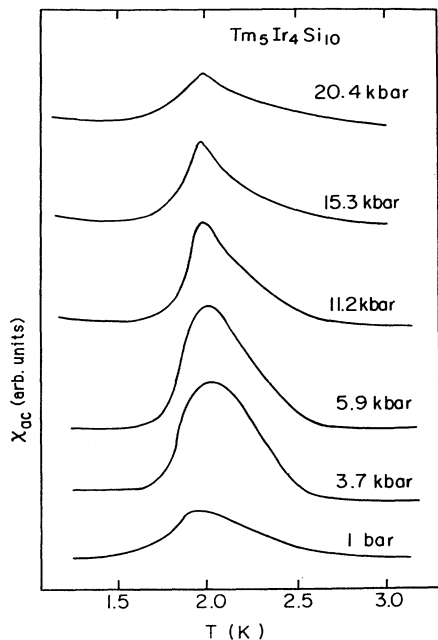


FIG. 6. χ_{ac} as a function of temperature between 1.2 and 3.2 K at six different pressures for $\text{Tm}_5\text{Ir}_4\text{Si}_{10}$.

two different types of magnetic transitions discussed in the last section as revealed in the ac magnetic susceptibility.

The heat capacity can be expressed as²³

$$C = C_n + C_m + C_e + C_l, \quad (2)$$

where C_n is the nuclear contribution. This nuclear Schottky anomaly arising from the interaction of the nu-

cleus with the effective magnetic field at the nucleus can be written as²³

$$C_n = A/T^2 \quad (3)$$

at temperatures well above the maximum in the total heat capacity. C_m is the magnetic contribution arising from the electrons in the unfilled 4f shell of the rare-earth ions. C_e is the usual electronic contribution, and C_l is the lattice contribution. In Fig. 9, we show the heat-capacity data for $\text{Tm}_5\text{Ir}_4\text{Si}_{10}$ from 1 to 10 K, where the solid line is fitted by the equation

$$C/R = A/T^2 + BT + DT^3 \quad (4)$$

in the range 4–10 K; here, R is the universal gas constant 8.314 J/mol K, and $A = 9.43 \text{ K}^2$, $B = 0.11 \text{ K}^{-1}$, and $D = 9.9 \times 10^{-5} \text{ K}^{-3}$ are obtained from the fit. A non-negligible nuclear Schottky contribution to the heat capacity is also seen in $\text{Sm}_2\text{Fe}_3\text{Si}_5$ and $\text{Ho}_2\text{Fe}_3\text{Si}_5$ ternary silicides.¹¹ Combining the results of $\text{Lu}_5\text{Ir}_4\text{Si}_{10}$,²⁴ $\gamma_n = 23.4 \text{ mJ/mol K}^2$, $\beta_n = 0.752 \text{ mJ/mol K}^4$, and $\alpha_n = 2.20 \times 10^{-3} \text{ mJ/mol K}^6$ fitted by

$$C = \gamma_n T + \beta_n T^3 + \alpha_n T^5 \quad (5)$$

and assuming the electronic and lattice contributions to the heat capacity of $\text{Tm}_5\text{Ir}_4\text{Si}_{10}$ are identical to those of $\text{Lu}_5\text{Ir}_4\text{Si}_{10}$, we can write the form of the magnetic contribution as

$$C_m/R = B'T + D'T^3. \quad (6)$$

Then $B' = 0.107 \text{ K}^{-1}$ and $D' = 9 \times 10^{-6} \text{ K}^{-3}$ are obtained in the range 4–10 K.

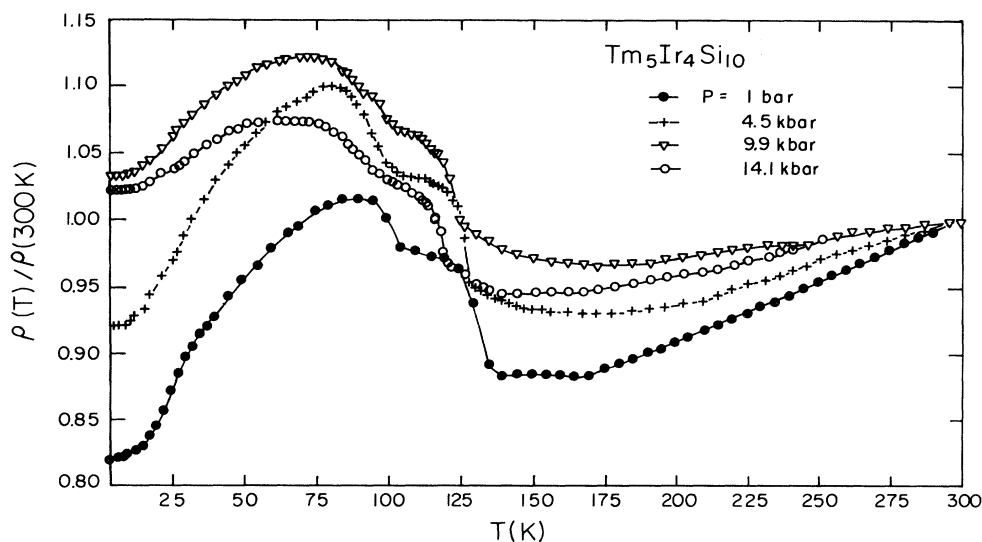


FIG. 7. Normalized resistivity as a function of temperatures between 4 and 300 K at four distinct pressures for $\text{Tm}_5\text{Ir}_4\text{Si}_{10}$.

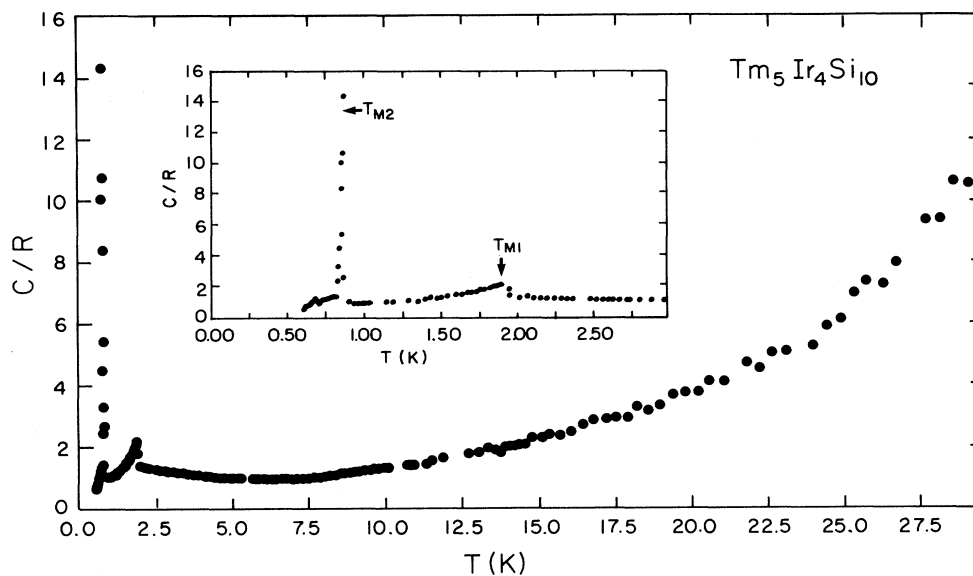


FIG. 8. Low-temperature heat capacity for $\text{Tm}_5\text{Ir}_4\text{Si}_{10}$ from 0.6 to 30 K. Inset shows data in the temperature range from 0.6 to 3 K.

IV. CONCLUSION

Measurements of the ac and dc magnetic susceptibility as a function of temperature have been performed for $R_5\text{Ir}_4\text{Si}_{10}$ ($R = \text{Dy} - \text{Yb}$) ternary silicides. All compounds, except $\text{Yb}_5\text{Ir}_4\text{Si}_{10}$, which is neither magnetic nor superconducting down to 52 mK, undergo magnetic transitions at very low temperature. Two magnetic transitions are found at 0.86 and 1.91 K for $\text{Tm}_5\text{Ir}_4\text{Si}_{10}$. Prob-

ably, one of these transitions is antiferromagnetic, while the other has a ferromagnetic component according to the ac-magnetic-susceptibility and heat-capacity data for this compound. Strong crystal-field effects or valence fluctuations are expected for $\text{Yb}_5\text{Ir}_4\text{Si}_{10}$ at low temperature ($T < 70$ K) because of the large deviation of the static magnetic susceptibility from the Curie-Weiss law. All compounds also exhibit an anomaly in the measurement of the resistivity versus temperature. Charge-density-

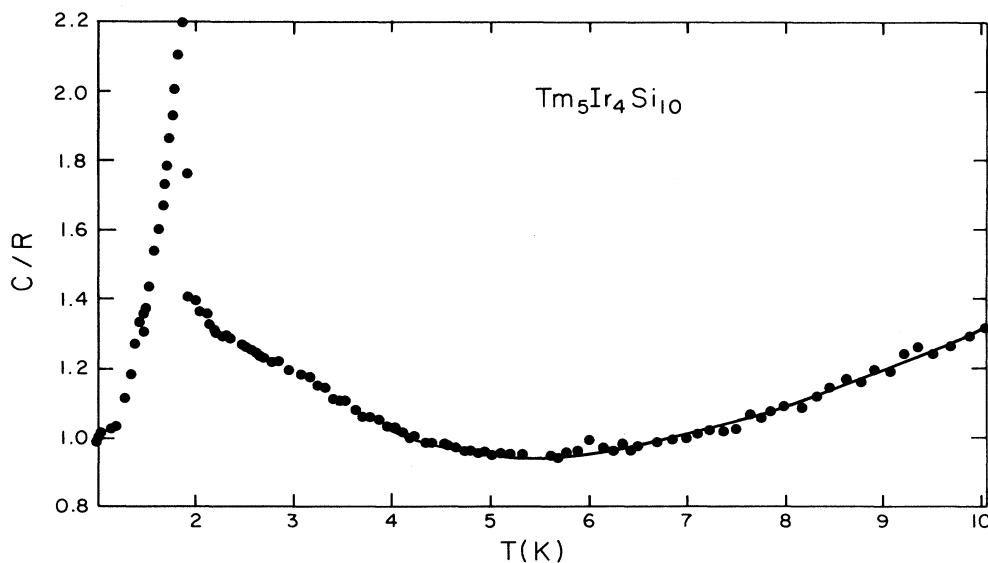


FIG. 9. Low-temperature heat capacity for $\text{Tm}_5\text{Ir}_4\text{Si}_{10}$ from 1 to 10 K. Solid line is a fit to $C/R = A/T^2 + BT + DT^3$ in the range 4–10 K.

wave formation, which was considered to occur in $\text{Lu}_5\text{Ir}_4\text{Si}_{10}$, is again thought to be the key reason giving rise to this anomaly.

ACKNOWLEDGMENTS

Research at National Sun Yat-sen University was supported by National Science Council Contract No.

NSC79-0208-M110-28. Research at the University of California, Davis, was supported by the National Science Foundation under Grant No. DMR-87-06117. Early stages of this work performed at the Ames Laboratory operated for the U.S. Department of Energy by Iowa State University under Contract No. W-7405-Eng-82 were supported by the Director for Energy Research, Office of Basic Energy Resources.

¹*Superconductivity in Ternary Compounds I and II*, edited by Ø. Fischer and M. B. Maple (Springer, New York, 1982).

²Ø. Fischer, *Appl. Phys.* **16**, 1 (1978).

³J. M. Vandenberg and B. T. Matthias, *Science* **198**, 194 (1978).

⁴H. F. Braun, *Phys. Lett.* **75A**, 386 (1980).

⁵H. F. Braun, C. U. Segre, F. Acker, M. Rosenberg, S. Dey, and P. Deppe, *J. Magn. Magn. Mater.* **25**, 117 (1981).

⁶H. F. Braun and C. U. Segre, *Solid State Commun.* **35**, 735 (1980).

⁷F. Steglich, J. Aarts, C. D. Bredl, W. Lieke, D. Meschede, W. Franz, and H. Schafer, *Phys. Rev. Lett.* **43**, 1982 (1979).

⁸C. U. Segre and H. F. Braun, in *Physics of Solids under High Pressure*, edited by J. S. Schilling and R. N. Shelton (North-Holland, Amsterdam, 1981), p. 381.

⁹C. U. Segre and H. F. Braun, *Phys. Lett.* **85A**, 372 (1981).

¹⁰C. B. Vining and R. N. Shelton, *Solid State Commun.* **54**, 53 (1985).

¹¹C. B. Vining and R. N. Shelton, *Phys. Rev. B* **28**, 2732 (1983).

¹²H. D. Yang, R. N. Shelton, and H. F. Braun, *Phys. Rev. B* **33**, 5062 (1986).

¹³R. N. Shelton, L. S. Hausermann-Berg, P. Klavins, H. D. Yang, M. S. Anderson, and C. A. Swenson, *Phys. Rev. B* **34**, 4590 (1986).

¹⁴H. F. Braun and C. U. Segre, in *Ternary Superconductors*,

edited by G. K. Shenoy, B. D. Dunlap, F. Y. Fradin (North-Holland, New York, 1981), p. 239.

¹⁵Quantum Design Inc., San Diego, CA.

¹⁶M. J. Johnson and R. N. Shelton, *Solid State Commun.* **52**, 839 (1984).

¹⁷C. B. Vining, R. N. Shelton, H. F. Braun, and M. Pelizzone, *Phys. Rev. B* **27**, 2800 (1983).

¹⁸H. F. Braun and M. Pelizzone, in *Superconductivity in d- and f-Band Metals*, edited by W. Buckel and W. Weber (Kernforschungszentrum, Karlsruhe, 1982), p. 245.

¹⁹H. D. Yang, P. Klavins, and R. N. Shelton, preceding paper, *Phys. Rev. B* **43**, 7681 (1991).

²⁰J. Chaussy, P. Haen, J. C. Lasjaunias, P. Monceau, G. Wayssand, A. Waintal, A. Meerschaut, P. Molinie, and J. Rouxel, *Solid State Commun.* **22**, 759 (1976).

²¹J. A. Wilson, F. J. DiSalvo, and S. Mahajan, *Adv. Phys.* **24**, 117 (1975).

²²P. M. Williams, G. S. Parry, and C. B. Scruby, *Philos. Mag.* **29**, 695 (1974).

²³L. J. Sundstorm, in *Handbook on the Physics and Chemistry of Rare Earths*, edited by K. A. Gschneidner, Jr. and L. Eyring (North-Holland, Amsterdam, 1978), Vol. 1, p. 379.

²⁴L. S. Hausermann-Berg and R. N. Shelton, *Phys. Rev. B* **35**, 6659 (1987).